IEEE Access
Multidisciplinary | Rapid Review | Open Access Journal

Received May 24, 2016, accepted June 26, 2016, date of publication June 28, 2016, date of current version July 22, 2016.

Digital Object Identifier 10.1109/ACCESS.2016.2585662

Reduced-Packet-Delay Generalized Buffer-Aided Relaying Protocol: Simultaneous Activation of Multiple Source-to-Relay Links

MIHARU OIWA, (Student Member, IEEE), AND SHINYA SUGIURA, (Senior Member, IEEE)
Department of Computer and Information Sciences, Tokyo University of Agriculture and Technology, Tokyo 184-8588, Japan

Corresponding author: S. Sugiura (sugiura@ieee.org)

This work was supported in part by the Japan Society for the Promotion of Science (JSPS) through the Grants-in-Aid for Scientific Research under Grant 26709028, and in part by the the Japan–Korea Basic Scientific Cooperation Program within JSPS and the National Research Foundation of Korea.

ABSTRACT Motivated by the recent buffer-aided relaying protocol that selects the best available link at each time slot, we herein introduce an additional degree of freedom to the protocol by simultaneously exploiting multiple links between the source node and the multiple buffer-aided relay nodes, which is enabled owing to the broadcast nature of wireless channels. More specifically, the proposed schemes are designed to allow multiple relay nodes to receive a source packet through source-to-relay broadcast channels, resulting in multiple copies of the source packet, which are stored in relay node buffers. As the explicit benefits of its increased design degree of freedom, the proposed protocols attain a significantly lower end-to-end packet delay than the conventional buffer-aided relaying protocols, which is achieved without imposing any substantial penalty on the achievable outage probability. Furthermore, the proposed protocol is capable of reducing the overhead required for monitoring the available links and buffer statuses of the relay nodes. Based on the Markov chain model, we derive the theoretical bounds of the outage probabilities of the proposed protocols.

INDEX TERMS Broadcast, buffers, cooperative communications, delay-tolerant network, Markov chain, outage probability, packet delay, spatial diversity.

I. INTRODUCTION

The recent concept of buffer-aided cooperative communications [1]–[16] allows us to attain a higher diversity gain than classic relaying schemes, which do not rely on buffers at relay nodes [17]–[20]. More specifically, the use of relay node buffers enables flexible scheduling of packet reception and transmission at relay nodes, enabling more beneficial link selection during each packet interval. Note that these benefits are achieved at the cost of imposing the additional overhead that is required for monitoring the statuses of all of the channels and for selecting the best available communication link. Another serious disadvantage of buffer-aided relaying schemes is the increase in end-to-end packet delay as a result of source packets being stored in a distributed manner at the relay nodes and relayed to the destination node in an unscheduled link selection process.

A number of buffer-aided relaying protocols have been proposed [1]–[5], [7]–[11], [13]–[15] for several cooperative network scenarios. A representative example is the max-max relay selection (MMRS) scheme [4], which uses two-phase packet transmissions for a two-hop multi-relay cooperative network. In the MMRS scheme, the relay node with the strongest source-to-relay (SR) channel is selected at each odd time slot, whereas the relay node with the strongest relay-to-destination (RD) channel is selected for packet transmission at each even time slot. This implies that the time slots for packet reception and transmission at relay nodes are scheduled in advance. In addition, the max-link protocol, in which the strongest available link is selected for transmission or reception at each time slot, was proposed in [5]. Since the max-link protocol has a higher number of degrees of freedom for link selection than its MMRS counterpart [4], the max-link protocol is capable of achieving higher diversity gain and a better outage probability. However, as demonstrated in [21], the max-link protocol's end-to-end packet delay is typically higher than that of the MMRS protocol for the practical scenario of finite source-packet transmissions. Most recently, a buffer-aided amplify-and-forward cooperative network was

developed in [11] based on the max-link relay-selection protocol. Moreover, an efficient buffer-aided bidirectional transmission strategy for block-fading channels was proposed in [22].

In previous buffer-aided relaying schemes, such as the MMRS [4] and max-link [5], [11] schemes, a single link is activated during each packet interval. For example, a packet transmitted from a source node is decoded and stored at a single selected relay node, although other relay nodes may be able to successfully decode the transmitted packet due to the broadcast nature of source-to-relay wireless channels. In this sense, previous buffer-aided cooperative schemes fail to make the best use of the SR broadcast channels. This is the primary motivation for the present study. In contrast, several multi-relay cooperation schemes that exploit the space-time coding gain [17], [19] or cyclic delay diversity [20] have been developed in order to attain a higher diversity gain. However, none of these schemes considers the use of buffers at the relay nodes. The milestones of the buffer-aided cooperative protocols are summarized in Table 1.

In addition, a major drawback of conventional buffer-aided cooperative protocols is the high overhead required for monitoring the channel state information (CSI) of all of the channels and the buffer states at relay nodes, as well as that for selecting an appropriate link. Most previous studies [4], [5], [9], [11] typically assumed that the destination node acts as a central coordinator and is in charge of these operations. This implies that the destination node must acquire the CSI of not only the RD links, but also that of the SR links that are not directly related to the destination node. Hence, the CSI of the SR channels must be periodically relayed to the destination node, which increases the overhead and the packet delay. Nevertheless, to the best of our knowledge, there have been no detailed investigations of the overhead associated with the link selection.

The novel contributions of the present study are as follows.[1]

[1] One of the two schemes proposed in this paper was originally introduced in our preliminary work [29], which demonstrated neither theoretical analysis of the outage probability, the comprehensive performance investigations, nor the comparisons of overhead and average packet delay between the existing and proposed schemes. Further novel contributions of this paper over [29] are highlighted below.

TABLE 1. Timeline of buffer-aided cooperative protocols.

Year	Authors	Contribution
2008	Xia *et al.* [1]	The authors showed that exploiting a data buffer at a relay node is capable of enhancing the throughput of a relay network.
2011	Mehta, Sharma, and Bansal [3]	The buffer-aided cooperative protocol using rateless codes was proposed, which ensures that both rate adaptation and relay selection occur without requiring instantaneous channel knowledge at the transmit source and relay nodes.
2012	Ikhlef, Michalopoulos, and Schober [4]	The authors introduced the MMRS protocol in the buffer-aided two-hop cooperative networks, which achieves a better outage probability than the conventional best-relay-selection cooperative protocol [23] that does not rely on buffers at relay nodes.
	Krikidis, Charalambous, and Thompson [5]	The max-link protocol was proposed for the buffer-aided two-hop cooperative networks, which is based on selecting the best available link in each time slot.
	Dong, Yang, and Hanzo [6]	The performance of multihop diversity in the buffer-aided multihop cooperative networks was analyzed.
	Ikhlef, Kim, and Schober [24]	Motivated by the MMRS protocol [4], a full-duplex buffer-aided cooperative protocol was proposed, where both a source and one of relay nodes are simultaneously activated to transmit packets.
2013	Liu *et al.* [8]	The concept of buffer-aided relaying protocols were extended to the case of two-way (bidirectional) relaying scenario, where the optimization problem for maximizing the sum rate was solved.
2014	Ahmed *et al.* [25]	The optimal power allocation scheme was presented for both the conventional and the buffer-aided link adaptive energy harvesting relay systems.
	Chen *et al.* [26]	The security of buffer-aided cooperative transmissions was considered, and a max-ratio relay selection protocol was proposed to offer the security transmission, while assuming the presence of an eavesdropper.
2015	Tian *et al.* [11]	An amplify-and-forward relay selection protocol was proposed in the context of buffer-aided cooperative systems.
	Dong *et al.* [13]	The authors provided comprehensive analysis of energy, delay, and outage probability for the buffer-aided three-node network.
	Jamali, Zlatanov, and Schober [27, 28]	The authors considered the bidirectional relay networks, where two users exchange information only via a relay node having a data buffer, and the both delay-unconstrained and delay-constrained protocols were proposed.
	Luo and Teh [15]	The authors proposed a buffer-state-based relay selection protocol for finite buffer-aided cooperative networks, which is capable of achieving lower average packet delay than the max-link protocol [5].
2016	Oiwa, Tosa, and Sugiura [21]	The hybrid buffer-aided cooperative protocol, exploiting both the benefits of the MMRS [4] and the max-link protocols [5], was proposed, in order to achieve a low outage probability as well as a low average packet delay.

- We introduce the concept of simultaneous use of multiple SR links into the framework of buffer-aided relaying protocols, in order to provide additional design degrees of freedom.[2] More specifically, we propose two novel buffer-aided relaying protocols, as the extensions of the previous MMRS and max–link protocols. Here, we refer to the two proposed schemes as generalized MMRS (G-MMRS) and generalized max-link (G-ML) protocols. Both of the proposed schemes are designed to allow a source node to transmit a packet to multiple relay nodes in a simultaneous manner, unless all SR channels are experiencing an outage. Then, multiple copies of the transmitted packet are used to attain a diversity gain in the relaying phase. As a result, the proposed schemes is capable of attaining the explicit benefits in terms of the end-to-end communication delay, which is achieved without requiring substantial buffer usage, as compared to conventional buffer-aided relaying protocols.
- The explicit benefit of the proposed G-MMRS protocol is that the overhead required for CSI acquisition is significantly reduced in comparison to the conventional MMRS and max-link protocols. More specifically, in the broadcast phase, the proposed G-MMRS protocol dispenses with any explicit link selection, and so the CSI of the SR channels is not needed at the destination node, whereas the conventional buffer-aided protocol must acquire the CSI of both the SR and RD channels. Consequently, in the proposed G-MMRS protocol, the number of channels that must be acquired at the destination node is half that of conventional MMRS protocol and quarter that of the conventional max–link protocol.
- The G-ML protocol, which is another one of the two proposed protocols, is capable of reducing the average end-to-end packet delay in comparison to the max-link protocol, while maintaining a good outage probability comparable to that of the max-link protocol. This implies that since the max-link protocol is designed for achieving the best maximum achievable diversity order, the G-ML protocol attains the same benefit.
- Furthermore, in the conventional studies of buffer-aided relaying protocols, any explicit comparisons of the overhead have not been provided. Hence, this paper provides overhead comparisons between the proposed and conventional buffer-aided protocols for the first time. Moreover, we derive the theoretical bound of outage probability of our proposed buffer-aided protocols, based on the Markov-chain model, where practical finite buffers are assumed for the relay nodes. Also, the average packet-delay bound was also derived for our buffer-aided protocols. Note that although in the previous studies of buffer-aided relaying protocols using a single link, the theoretical analysis of the outage probability and the average packet delay has been carried out, it is not applicable to our novel multi-link activation counterpart due to the difference of the system models.

[2]In the clssic cooperative communiation schemes, which do not rely on the buffers at relay nodes, the simultaneous exploitation of multiple SR links is typically considered. By contrast, in the recent buffer-aided cooperative scenario, which is focused on in this paper, the use of broadcast nature of the multiple SR links has been unexplored, and hence its detailed investigations are our main controbutions.

The remainder of the present paper is organized as follows. In Section II, we present a model of the proposed buffer-aided cooperative scheme, and the overhead imposed by the link selection operation is evaluated in Section III. In Section IV, we derive the theoretical outage probability. In Section V, the theoretical average packet delay is provided. In Section VI, we present the obtained performance results, and we present our conclusions in Section VII.

II. SYSTEM MODEL

Let us consider a two-hop relaying network consisting of a single source node, K relay nodes, and a single destination node, where the kth relay node is equipped with a buffer Q_k of finite size L, and the number of packets stored at the kth relay node is represented by $\Psi(Q_k)$ $(0 \leq \Psi(Q_k) \leq L)$. We assume that no direct link exists between the source and destination nodes and that all of the nodes operate in half-duplex mode under a decode-and-forward principle. This means that at least two time slots are required for each end-to-end packet transmission. The transmission rate of each node is maintained to be constant at r_0 bps/Hz, and so the effective overall transmission rate is upper-bounded by $r_0/2$ bps/Hz. Moreover, we assume that there are stable low-rate feedback channels, where acknowledge (ACK) packets are transmitted from the destination node to the relay nodes.

Throughout the present paper, we consider independent, identically distributed (IID) Rayleigh fading channels for all the SR and RD links, having the same SNR value γ. Note that this simplified assumption of symmetric channels was typically used in previous studies, although this scenario is readily extended to asymmetric counterparts. Here, the frequency-flat channel coefficient of the kth SR channel is denoted by h_{SR_k}, whereas that of the kth RD channel is given by h_{RD_k}. Moreover, the capacity associated with channel $h_\bullet$ is represented by $\mathcal{C}(h_\bullet)$.

A. THE CONVENTIONAL MMRS PROTOCOL [4]

In the conventional MMRS protocol [4], the time slots used for the SR and the RD transmissions are scheduled in advance. In each odd time slot, the single strongest one out of the K SR links is selected for the transmission of a source packet. Here, if the transmission rate is lower than the channel capacity associated with the selected SR link, the source packet is allowed to be transmitted. Otherwise, the selected link experiences an outage event. Similarly, in each even time slot, the single strongest one out of the K RD links is selected, and if it does not experience an outage, the packet at the selected relay is transmitted. Again, the conventional MMRS protocol activates only a single link in each time slot.

The advantage of the MMRS protocol is that the CSI update is once per two time slots, which is half of that of

the max-link protocol. However, the MMRS protocol fails to attain the maximum achievable diversity order, since at each time slot, the number of available links is K, rather than $2K$. The outage probability of the MMRS protocol was estimated in [4] under the idealistic assumption that the buffer selected for reception (transmission) is not full (empty). Hence, the effects of the status of the buffers at the relays were not taken into account, and hence the outage probability derived in [4] is overestimated. More recently, in [21] the outage probability of the MMRS protocol with finite-buffer relays was derived, based on the analysis of the periodic Markov chain.

B. THE CONVENTIONAL MAX–LINK PROTOCOL [5]

Aiming for combating the above-mentioned limitation of the MMRS protocol, the max–link protocol was designed to select the strongest link out of all the available SR and RD links in each time slot. Hence, the maximum achievable diversity order corresponds to the total number of SR and RD links, assuming that all the buffers are not either full or empty. This maximum achievable diversity order is twice that of the MMRS protocol. In the max–link protocol, the number of activated links per time slot is one, similar to the conventional MMRS protocol.

The theoretical outage probability for the max–link protocol with finite buffers was derived in [5]. Here, the status of the buffers was modeled by an aperiodic Markov chain, and both the steady-state probability and the corresponding outage probability were formulated.

C. THE PROPOSED G-MMRS PROTOCOL

In this section, we describe the proposed buffer-aided G-MMRS protocol. Fig. 1 shows the schematic of the proposed two-phase G-MMRS protocol. Similar to the conventional MMRS protocol [4], the transmissions of the G-MMRS protocol are divided into two phases, namely, the broadcast phase in odd time slots and the relaying phase in even time slots, which are shown in Figs. 1(a) and 1(b), respectively.

In the broadcast phase, the source node broadcasts a source packet to the relay nodes over the broadcast channels between the source node and the relay nodes. More specifically, the source packet is stored in the buffers of subset $\mathcal{R}$ of K relay nodes, which is represented as follows:

$$\mathcal{R} = \{R_k \mid \mathcal{C}(h_{\mathrm{SR}_k}) > r_0 \ \cap \ \Psi(Q_k) \neq L\}, \tag{1}$$

where $\mathcal{C}(h_{\mathrm{SR}_k})$ is the channel capacity between the source node and the kth relay node, which is given by

$$\mathcal{C}(h_{\mathrm{SR}_k}) = \frac{1}{2}\log_2\left(1+\gamma\left|h_{\mathrm{SR}_k}\right|^2\right). \tag{2}$$

If the buffers of all of the relay nodes are full, or if there is no SR link having a higher capacity than the transmission rate r_0, the corresponding broadcast phase is counted as an outage event. Note that in (1), we assume that when the channel capacity is higher than the transmission rate, the packet is successfully decoded at the corresponding relay node with the aid of a capacity-achieving channel coding scheme, such as turbo or low-density parity-check codes [30]. Note also that source packets are encoded by cyclic redundancy check (CRC) codes, and so the relay nodes are capable of autonomously judging whether the decoded packets include an error. This indicates that no explicit SR link selections or associated channel monitoring are needed in this broadcast phase. This is one of the explicit benefits compared to conventional buffer-aided link selection schemes, such as the MMRS scheme and the max-link scheme, which requires a substantial overhead to monitor all of the SR channels.

In the relaying phase of Fig. 1(b), a local coordinator selects a single relay node that is allowed to transmit a packet to the destination node. More specifically, the selected relay node has the strongest RD channel among the relay nodes that have at least one packet in their buffers. Here, the best selected relay node R_{best} is given as follows:

$$R_{\mathrm{best}} = \arg\max_{R_k}\left\{\bigcup_{R_k:\Psi(Q_k)\neq 0}\left(\left|h_{\mathrm{RD}_k}\right|^2\right)\right\}. \tag{3}$$

Note that the relay node transmits from the queued packets in a first-come, first-served manner. After the destination node receives the relayed packet, an ACK packet is sent to all of the relay nodes through stable low-rate feedback channels. The corresponding packet copied at the relay nodes is then

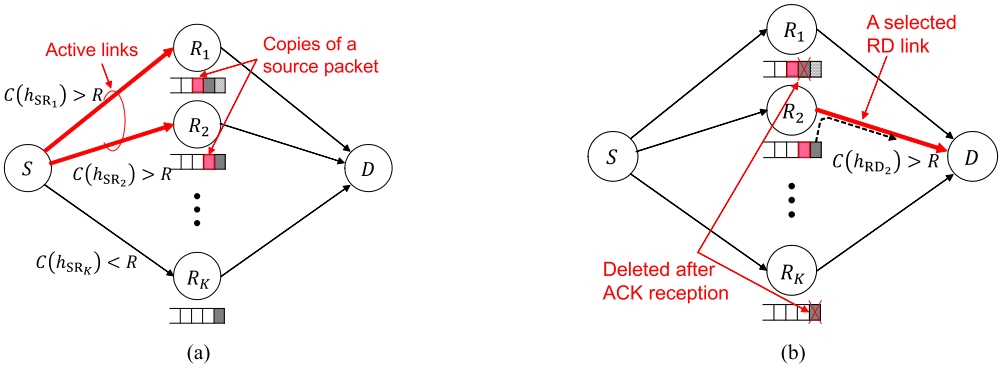

FIGURE 1. System model of the proposed G-MMRS protocol, which exploits multiple active links at the broadcast phase in a simultaneous manner. (a) Broadcast phase. (b) Relaying phase.

deleted from the buffers, as shown in Fig. 1(b). Note that, in this sense, the relay-selection criterion in the relaying phase is the same as that of the conventional MMRS protocol, whereas sending the ACK packet to all of the relays is specific to the proposed protocol. Clearly, the proposed G-MMRS scheme has the explicit advantage of attaining a higher spatial diversity gain in the relaying phase as compared to the conventional MMRS scheme, because multiple copies of source packets tend to be stored at different relay nodes, providing a higher number of chances for the destination node to attain the packet.

D. THE PROPOSED G-ML PROTOCOL

In this section, we present another proposed buffer-aided protocol, i.e., the G-ML protocol, where the conventional max–link protocol is generalized to include the concept of our multiple SR link activation.

More specifically, in the G-ML protocol, one out of all $2K$ links is selected in each time slot. If the selected link is an SR link, then the source node broadcast a source packet to all the K relay nodes, which becomes exactly the same as the broadcast phase of the G-MMRS protocol, shown in Fig. 1(a). If the selected link is an RD link, the single selected relay node transmits the packet stored in its buffer to the destination node, in a similar manner to the relaying phase of G-MMRS protocol of Fig. 1(b). It is explicit that in our G-ML protocol the number of available links increases in comparison to that of the conventional max–link counterpart, when the strongest link is an SR link.

Additionally, it is predicted that when the SR and RD channels are asymmetric, i.e., non-identically distributed, there tends to be a buffer overflow or an empty buffer at each relay node in the G-ML protocol, similar to the conventional max-link protocol [10], and hence the appropriate modifications are needed for combating this limitation. To this end, we propose an optional scheme of the G-ML protocol, which is referred to as *the balanced G-ML protocol* in this paper.

Let us introduce a percentage P_C [10], [31], which is used for balancing the link selection in the balanced G-ML protocol. When there are SR and RD links that are not in outage, broadcast SR links are activated in the $(100 - P_C)$ percentage of time slots, and a RD link is selected in the P_C percentage of time slots. This enables us to avoid keeping selecting only either SR or RD links in our balanced G-ML protocol.

E. REDUCED AVERAGE END-TO-END PACKET DELAY

Another benefit of the two protocols proposed in Sections II-C and II-D is that the average end-to-end packet delay is significantly reduced as compared to conventional buffer-aided relaying schemes. As an explicit example, let us consider the scenario in which the SNRs of all of the SR channels are sufficiently high. In the G-MMRS protocol, source packets broadcast from the source node are copied at the buffers of all of the relay nodes. Considering that the packets stored at the relay nodes are transmitted in a first-come, first-served fashion, regardless of which relay node is selected in the relaying phase of Fig. 1(b), the order of the packets received at the destination node is the same as the order of the original source packets. In general, the same reduced-delay advantage of the proposed protocol holds true in other SNR regimes.

In contrast, in the conventional MMRS protocol, source packets are distributed over the buffers of the relay nodes, where each packet is queued in the buffer of a single relay node. Since the RD link selection process is random, the order of the packets received at the destination node tends to be random, depending on the selected relay node. This causes an increase in the average end-to-end packet delay. Similarly, the same discussion holds true for the relationship between the proposed G-ML and the conventional max–link protocols, where the G-ML protocol tends to exhibit a lower packet delay profile than the max–link protocol. In Section VI-C, the simulation results of the present study clarify the effects of the reduced packet delay of the proposed protocols.

F. ENERGY CONSUMPTION

Let us compare the energy consumption of the relay nodes in the conventional and the proposed buffer-aided protocols. As mentioned in [32], the total energy consumption includes both the transmission energy and the circuit energy consumption. In the previous studies on the energy-efficient communications, the transmission energy consumption is typically focused on, since it is the dominant factor in the total energy consumption. This is especially true when considering the long-range applications.[3]

Furthermore, for the relaying phase of all the four conventional and proposed protocols, introduced in Sections II-A–II-D, only a single relay node is selected for transmitting a packet stored in its buffer. Hence, the transmission energy consumptions of the four protocols are similar. In contrast, for the source-transmission phase, multiple relay nodes are activated for receiving a source packet in the proposed G-MMRS and G-ML protocols, while only a single relay node is active in the conventional MMRS and max-link protocols, where other inactive relay nodes may be silent in the associated packet interval. It may be possible that the circuit energy consumption of the conventional protocols may be reduced, by turning off the inactive relay nodes. However, its impact on the total energy consumption is limited, due to the reason mentioned above. The detailed investigations are out of the scope of this paper, which are left for the future studies.

[3]Note that in the short-range applications, such as sensor networks, the circuit energy consumption may be comparable to the transmission energy consumption. However, the channel's coherence time is typically long in such a scenario, which is not beneficial for the buffer-aided cooperative protocols, as shown in our performance results provided in Section VI. Hence, the short-range applications are not the main focus of this paper.

TABLE 2. Required overheads of the proposed scheme, the MMRS scheme, and the max-link scheme for the destination node to monitor CSI and buffer states per link selection (time slot).

	Pilot transmissions		CSI estimations		Data transmissions from relay nodes	
	source node	each relay node	each relay node	destination node	CSI of SR links	buffer states
Proposed G-MMRS	0	$1/2$	0	$K/2$	0	$K/2$
Proposed G-ML	1	1	1	K	K	K
Conventional MMRS [4]	$1/2$	$1/2$	$1/2$	$K/2$	$K/2$	K
Conventional max-link [5]	1	1	1	K	K	K

III. OVERHEAD REQUIRED FOR MONITORING CSI AND BUFFER STATES

In this section, we evaluate the additional overhead required for the link selection, which has not been investigated in previous studies. Here, we compare the overheads of the proposed protocols and the conventional MMRS and max-link protocols. More specifically, we herein focus on the overhead required for a central coordinator to monitor the CSI and buffer states of the relay nodes, which are used to select an appropriate link at each time slot. We assume that the destination node acts as a central coordinator, in a similar manner to most of the previous studies [4], [5], [9], [11], and that the channels remain constant over the link selection and the packet transmission. This corresponds to the quasi-static fading scenario.

The overheads are shown in Table 2, which lists the number of pilot transmissions, the estimated CSI, and the data transmissions, all per time slot (i.e., per link selection). First, the overhead imposed on the max-link protocol per link selection was characterized as follows. In the max-link protocol, all of the SR and RD channels, as well as the buffer states of the relay nodes, must be updated at the destination node for each time slot, i.e., in advance of each link selection. To this end, the source node broadcasts a pilot block to the K relay nodes, and each relay node carries out CSI estimation based on the received pilot block. Then, the CSI of the kth SR channel, estimated at the kth relay node, is transmitted to the destination node together with the buffer state of the kth relay node. Next, each relay node transmits a pilot block to the destination node, and the destination node then estimates the CSI of the K RD links, based on the K pilot blocks.

Next, let us consider the overhead imposed on the MMRS protocol per time slot. In the MMRS protocol, the link selections of the SR and RD links are separated, depending on odd or even time slots. For instance, SR-link selection is performed once for every two time slots. Hence, in the MMRS protocol, CSI updating of the SR channels at the destination node is also performed once for every two time slots, in contrast to that in the max-link protocol, which has to be carried out once for every time slot. Similarly, the CSI update of the RD channels in the MMRS protocol is half that of the max-link protocol. As for updating of the buffer states, the overhead of the MMRS protocol is the same as that of the max-link protocol, because the buffer states are used for the link selection at both the odd and even time slots of the MMRS protocol. Consequently, as shown in Table 2, the overhead of the MMRS protocol is half that of the max-link protocol, except for the overhead associated with the buffer states of the relay nodes.

Furthermore, we evaluate the overhead imposed on the proposed G-MMRS protocol, which is pre-scheduled for odd and even time slots, similar to the MMRS protocol. More specifically, the G-MMRS protocol does not relay on any link selection at odd time slots, thereby dispensing with the CSI of the SR links. In contrast, the proposed protocol's RD link selection at even time slots is the same as that of the conventional MMRS protocol. Table 2 shows that the proposed G-MMRS protocol attained an overhead that was approximately twice and four times lower than the overheads of the conventional MMRS and max-link protocols, respectively. In order to provide further insights, in a fast-fading scenario, in which the coherence time of the channel is shorter than the time-slot duration, the CSI update must be more frequent than once per time-slot duration. Otherwise, link selections are carried out based on inaccurate CSI, which degrades the achievable performance of the buffer-aided cooperation. In such a fast-fading scenario, the advantage of the proposed G-MMRS scheme may become more explicit because, unlike in other buffer-aided cooperative schemes, the SR channels in the proposed protocol, which are indirect for the destination node, do not have to be monitored.

Finally, we characterize the overhead of the proposed G-ML protocol. Since the link selection process of the G-ML protocol is similar to the conventional max–link protocol except for the exploitation of multiple SR links, the overhead of the two schemes is the same, as shown in Table. 2.

Note that in the overhead evaluations of Table 2, it is assumed for simplicity that the buffers of relay nodes are neither empty nor full. However, since the empty- and full-buffer relay node cannot transmit and receive a packet, the overhead associated with the RD and SR CSI may be reduced, respectively. For example, a relay node having an empty buffer does not have the possibility of being selected as a transmit relay, and hence the related RD CSI does not have to be updated at the destination node, while its SR CSI has to be relayed to the destination node as usual. Similarly, a relay node having a full buffer is not required to relay its SR CSI to the destination node. Importantly, since this overhead reduction scheme is applicable to all the four protocols

in Table 2, the advantage of the proposed G-MMRS and G-ML protocols remains unchanged.[4]

IV. THEORETICAL ANALYSIS OF OUTAGE PROBABILITY

In this section, we derive the theoretical outage probability of the two proposed schemes based on the Markov-chain model, which takes into account the effects of finite-size buffers at relay nodes. Moreover, we assume that sufficiently long packets are transmitted from the source node to the destination node. For the sake of simplicity, we focus on a specific scenario of $K = 2$ relay nodes, each having an $(L = 2)$-sized buffer. However, the analytical framework derived in this section is readily applicable to the system configuration supporting an arbitrary (K, L) set. Note that the theoretical outage probability considering finite buffers at relay nodes has been derived for the max-link protocol in [5], where the steady-state probabilities are calculated by modeling the buffer states as an ergodic Markov chain. However, the analytical framework derived in [5] is not directly applicable to the two proposed schemes due to the existence of two fundamental differences between the two schemes. First, the two proposed schemes are designed to allow a specific source packet to be stored at buffers of different relay nodes, whereas, in the conventional max-link and MMRS protocols, each source packet is stored at a single relay node. This imposes an increase in the number of states associated with the Markov model on the proposed scheme. Second, the proposed G-MMRS scheme includes two different link-activation processes, i.e., the multiple SR-channel activation in the broadcast phase and the maximum RD link selection in the relaying phase, which leads to the periodic Markov model depending on odd or even time slots. Note that the Markov model of the G-MMRS protocol is periodic, which implies that in order to determine the analytical steady states, as well as the outage probability, the Markov chain process of the proposed G-MMRS protocol must be considered separately for odd and even time slots.

A. THE OUTAGE BOUND OF THE G-MMRS PROTOCOL

Now, let us introduce the Markov chain model that is valid specifically for the proposed G-MMRS scheme. The legitimate buffer states are listed in Table 3, where we have $N_{\text{state}} = 19$ total number of states. Here, in the first nine states s_i $(i = 1, \cdots, 9)$, a specific packet is not shared at the $K = 2$ relay nodes, which corresponds to the conventional max-link and MMRS schemes. In contrast, the latter ten states s_i $(i = 10, \cdots, 19)$ allow multiple copies of the source packets at different relay nodes, which are the conditions specific to the proposed protocol.[5]

[4]Furthermore, as shown in Table 4, the ratio of the relay nodes having empty or full buffers is not high, and hence the effects of this overhead reduction are limited.

[5]Without loss of generality, in order to represent Markov-chain states of our scheme, we only have to consider the legitimate combinations of packets stored at buffers [21], rather than their permutations.

TABLE 3. Relationship between Markov-chain states and buffers of $K = 2$ relay nodes, each having an $(L = 2)$-sized buffer.

States	Relay 1		Relay 2	
	buffer 1	buffer 2	buffer 1	buffer 2
s_1	empty	empty	empty	empty
s_2	◯	empty	empty	empty
s_3	empty	empty	◯	empty
s_4	◯	□	empty	empty
s_5	◯	empty	□	empty
s_6	empty	empty	◯	□
s_7	◯	△	□	empty
s_8	◯	empty	□	△
s_9	◯	△	□	◇
s_{10}	◯	empty	◯	empty
s_{11}	◯	△	◯	empty
s_{12}	◯	empty	◯	△
s_{13}	◯	△	◯	△
s_{14}	◯	△	◯	□
s_{15}	◯	empty	□	◯
s_{16}	◯	△	□	◯
s_{17}	□	◯	◯	empty
s_{18}	□	◯	◯	△
s_{19}	□	◯	△	◯

◯, △, ◇, □ represent four different packets

Furthermore, the state diagrams of the Markov chain for odd and even time slots are shown in Figs. 2(a) and 2(b), respectively. In the diagrams, the red arrows indicate outage events, where each state remains the same after a single transition. The black solid arrows represent the transitions associated with successful packet transmissions from the source or relay nodes. Let us consider the transition matrix $\mathbf{A}_{\text{odd}} \in \mathbb{R}^{N_{\text{state}} \times N_{\text{state}}}$ for an odd time slot, where the jth-row and ith-column element of $\mathbf{A}_{\text{odd}}$ corresponds to the transition probability from the ith state s_i to the jth state s_j at an odd time slot. Similarly, the transition matrix $\mathbf{A}_{\text{even}} \in \mathbb{R}^{N_{\text{state}} \times N_{\text{state}}}$ represents the transition matrix at an even time slot.

More specifically, the transition probabilities contained in the matrices $\mathbf{A}_{\text{odd}}$ and $\mathbf{A}_{\text{even}}$, which are calculated from the following formulas, are specified in Fig. 2:

$$p_D = \frac{1}{D}\left[1 - \left(1 - \exp\left(-\frac{2^{2R}-1}{\gamma}\right)\right)^D\right], \quad (4)$$

$$\bar{p}_D = \left(1 - \exp\left(-\frac{2^{2R}-1}{\gamma}\right)\right)^D, \quad (5)$$

$$p_{\text{e}} = \exp\left(-\frac{2^{2R}-1}{\gamma}\right), \quad (6)$$

$$\hat{p}_D = p_{\text{e}}\bar{p}_{D-1}, \quad (7)$$

$$\Phi(a, b) = \sum_{i=0}^{b} \binom{b}{i} p_{\text{e}}^i (1 - p_{\text{e}})^{b-i} \frac{a}{a+i}, \quad (8)$$

where p_D represents the probability of having at least one specific available link from D links, and $\bar{p}_D$ denotes the

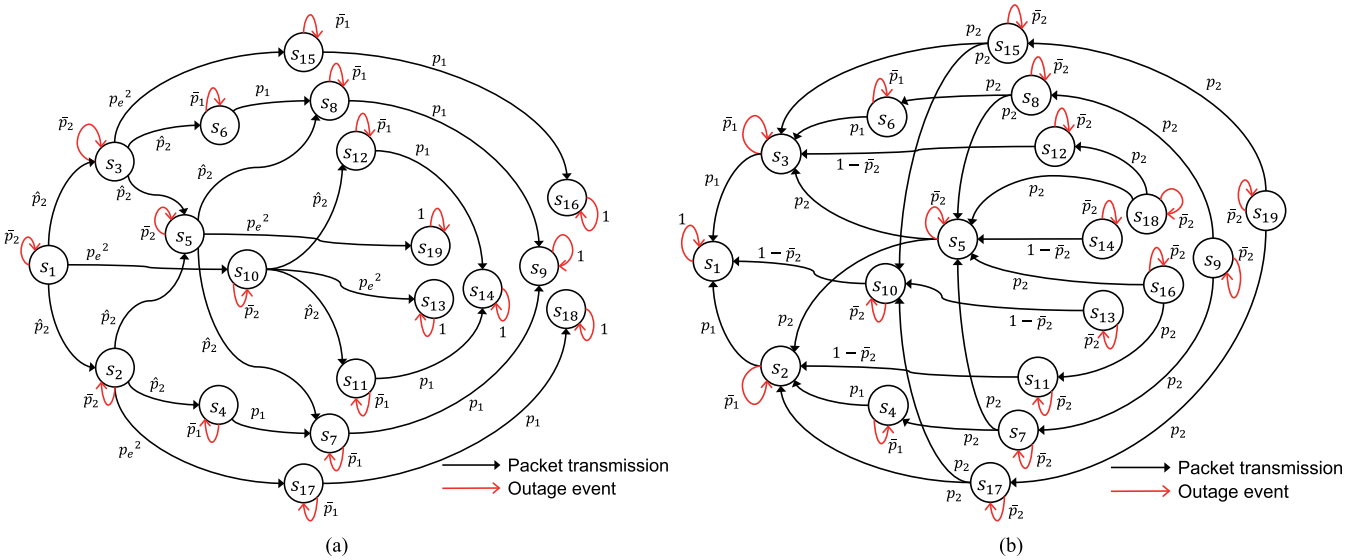

FIGURE 2. State diagram of the Markov chain model representing the proposed G-MMRS scheme with $K = 2$ relay nodes, each having a buffer of size ($L = 2$). (a) Odd time slot (broadcast phase) and (b) even time slot (relaying phase).

probability that all of the links (D) are in the outage state. Furthermore, p_e is the probability that a single specific link is not in the outage state, whereas $\hat{p}_D$ is the probability that a specific link is available and the other $D-1$ links are in the outage state.

For example, consider the transition from state s_5 to state s_8 at an odd time slot, i.e., in a broadcast phase, as shown in Fig. 2(a). According to Table 3, this transition occurs when the link between the source node and the first relay node is in an outage state and when the link between the source node and the second relay node is not in an outage state. This probability corresponds to the probability $\hat{p}_2$ formulated by (7). Similarly, the transitions shown in Fig. 2 are expressed by (4) through (7).

A state transition from a specific odd time slot to the next odd time slot is represented by the transition matrix of $\mathbf{A}_{\text{even}}\mathbf{A}_{\text{odd}}$. Then, in order to calculate a unique steady-state probability $\boldsymbol{\pi}_{\text{odd}} = [\pi_{\text{odd},1}, \cdots, \pi_{\text{odd},N_{\text{state}}}]^T \in \mathbb{R}^{N_{\text{state}}}$, which is valid for odd time slots, the following equations must be satisfied:

$$\boldsymbol{\pi}_{\text{odd}} = \mathbf{A}_{\text{even}}\mathbf{A}_{\text{odd}}\boldsymbol{\pi}_{\text{odd}} \tag{9}$$

$$\sum_{i=1}^{N_{\text{state}}} \pi_{\text{odd},i} = 1. \tag{10}$$

Moreover, (10) may be expressed as follows:

$$\mathbf{B}\boldsymbol{\pi}_{\text{odd}} = \mathbf{b}. \tag{11}$$

Here, we have $\mathbf{b} = [1, \cdots, 1]^T \in \mathbb{R}^{N_{\text{state}}}$ and $\mathbf{B} = [\mathbf{b}, \cdots, \mathbf{b}] \in \mathbb{R}^{N_{\text{state}} \times N_{\text{state}}}$. Then, based on (9) and (11), we obtain

$$\boldsymbol{\pi}_{\text{odd}} = (\mathbf{A}_{\text{even}}\mathbf{A}_{\text{odd}} - \mathbf{I} + \mathbf{B})^{-1}\mathbf{b} \in \mathbb{R}^{N_{\text{state}}}, \tag{12}$$

where $\mathbf{I} \in \mathbb{R}^{N_{\text{state}} \times N_{\text{state}}}$ is the identity matrix.

In a similar manner to the derivation of (12), the steady-state probabilities for even time slots are formulated as follows:

$$\boldsymbol{\pi}_{\text{even}} = (\mathbf{A}_{\text{odd}}\mathbf{A}_{\text{even}} - \mathbf{I} + \mathbf{B})^{-1}\mathbf{b} \in \mathbb{R}^{N_{\text{state}}}. \tag{13}$$

Let us introduce a theoretical bound of the proposed protocol's outage probability based on the steady-state probabilities at odd and even time slots, which are formulated in (12) and (13). Considering that an outage event occurs when there is no change in the status of the buffers, the corresponding outage probability is given by

$$P_{\text{out}} = \frac{1}{2}\sum_{i=1}^{N_{\text{state}}} \left(\pi_{\text{odd},i}[\mathbf{A}_{\text{odd}}]_{ii} + \pi_{\text{even},i}[\mathbf{A}_{\text{even}}]_{ii}\right) \tag{14}$$

$$= \frac{1}{2}\text{diag}(\mathbf{A}_{\text{odd}})\boldsymbol{\pi}_{\text{odd}} + \frac{1}{2}\text{diag}(\mathbf{A}_{\text{even}})\boldsymbol{\pi}_{\text{even}}, \tag{15}$$

where $[\mathbf{A}]_{ii}$ represents the ith-row and ith-column element of a matrix $\mathbf{A}$, and $\pi_{\text{odd},i}$ and $\pi_{\text{even},i}$ denote the ith elements of vectors $\boldsymbol{\pi}_{\text{odd}}$ and $\boldsymbol{\pi}_{\text{even}}$, respectively.

B. THE OUTAGE BOUND OF THE G-ML PROTOCOL

Having provided the theoretical outage probability bound of the G-MMRS protocol, let us also derive that of the proposed G-ML protocol. Since the Markov chain of the G-ML protocol is aperiodic, similar to the conventional max–link protocol, it is expressed by a single model. More specifically, Fig. 3 shows the state diagram of the Markov model of the proposed G-ML protocol, while considering $K = 2$ relay nodes, each having a buffer of $L = 2$. Here, each of the transition probabilities shown in Fig. 3 is expressed by (4)–(8), similar to the G-MMRS case of Section IV-A.

By defining $\mathbf{A} \in \mathbb{R}^{N_{\text{state}} \times N_{\text{state}}}$ as the transition matrix of the Markov model of Fig. 3, the steady state probabilities

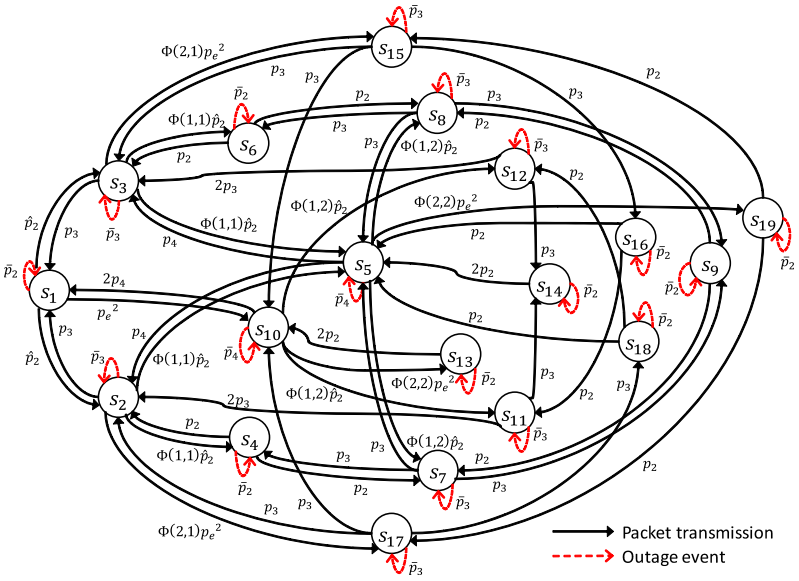

FIGURE 3. State diagram of the Markov chain model representing the proposed G-ML scheme with $K = 2$ relay nodes, each having a buffer of size ($L = 2$).

$\boldsymbol{\pi} \in \mathbb{R}^{N_{\text{state}}}$ are constituted in a closed-form as

$$\boldsymbol{\pi} = (\mathbf{A} - \mathbf{I} + \mathbf{B})^{-1}\mathbf{b} \in \mathbb{R}^{N_{\text{state}}}. \tag{16}$$

Note that in the proposed G-ML protocol, the transition and the legitimate number of states are different from those of the conventional max–link protocol [5].

Finally, the theoretical outage probability bound is formulated according to [5] as follows:

$$P_{\text{out}} = \text{diag}(\mathbf{A})\boldsymbol{\pi}. \tag{17}$$

V. THEORETICAL BOUND OF AVERAGE END-TO-END PACKET DELAY

In this section, we provide the average packet-delay bounds of the proposed G-ML and G-MMRS protocols. According to the previous studies [7], [11], [13], [21], we employ the simplified assumptions of infinite source-packet transmissions and finite-buffer relay nodes.[6]

From Little's law [33], the average delay at the kth relay node is given by

$$\mathbb{E}[T_k] = \frac{\mathbb{E}[\Psi(Q_k)]}{\eta_k}, \tag{18}$$

where η_k is the average throughput at the kth relay node. Note that since the probabilities of selecting any of the relay nodes are identical [11], the average packet delay of each relay node is also the same as (18).

[6]Note that in [7] and [13] the average packet-delay analysis was provided for a simple three-node buffer-aided network, while that of the multiple-relay networks was provided for the max-link, the MMRS, and their hybrid protocols in [21]. Furthermore, in [11] the theoretical delay analysis was provided for the multiple-relay amplify-and-forward buffer-aided protocol.

More specifically, (18) is modified to

$$\mathbb{E}[T_k] = \frac{\sum_{i=1}^{N_{\text{state}}} \pi_i \Psi(Q_k(i))}{\sum_{i=1}^{N_{\text{state}}} \sum_{j=1}^{K} \pi_i p_{kj}(i)}, \tag{19}$$

where π_i is the ith state of $\boldsymbol{\pi}$, and $\Psi(Q_k(i))$ represents the number of packets stored at the kth relay node for the state π_i. Furthermore, $p_{kj}(i)$ is the probability that a packet stored at the kth relay node is reduced by selecting the jth RD link.

In order to elaborate a little further, let us consider the scenario where the jth and the kth relay nodes have the same specific packet in their buffers. Then, if the jth relay node transmits the packet to the destination node, the same packet stored in the buffer of the kth relay is also deleted, which is the situation specific to the proposed G-MMRS and G-ML protocols.

The average packet-delay bound of (19) may have a small gap from the numerical results. This is because the packet flow of the proposed protocols may not operate in a fast-in fast out manner, where the effects are not taken into account in (19).

VI. PERFORMANCE RESULTS

In this section, we present our theoretical and simulation results in order to characterize the proposed G-MMRS and G-ML protocols. The transmission rate r_0 of each node was set to $r_0 = 1$ bps/Hz. The buffers at all of the relay nodes were set to empty in the initial condition of each Monte Carlo simulation. We assumed that all of the SR and RD channels are generated at each time slot. The max-link and the MMRS protocols were chosen as the benchmark schemes.

A. OUTAGE PROBABILITY

Here, we evaluated the outage probability, where we considered sufficiently long source packets to be transmitted

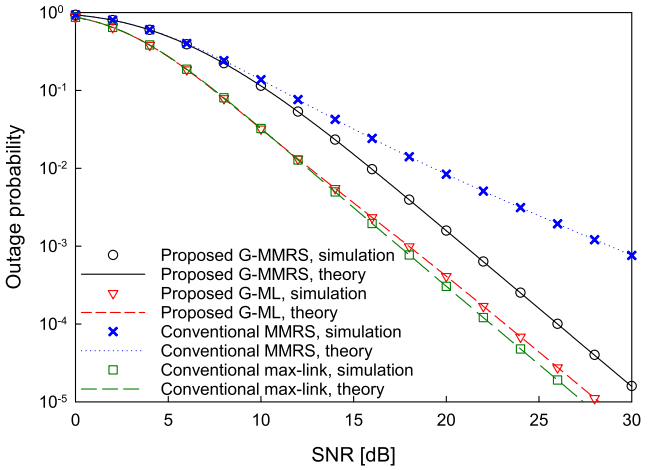

FIGURE 4. Theoretical and numerical outage probabilities of the proposed G-MMRS and G-ML schemes, having $K = 2$ relay nodes, each having an ($L = 2$)-sized buffer, while plotting those of the conventional MMRS and max–link counterparts.

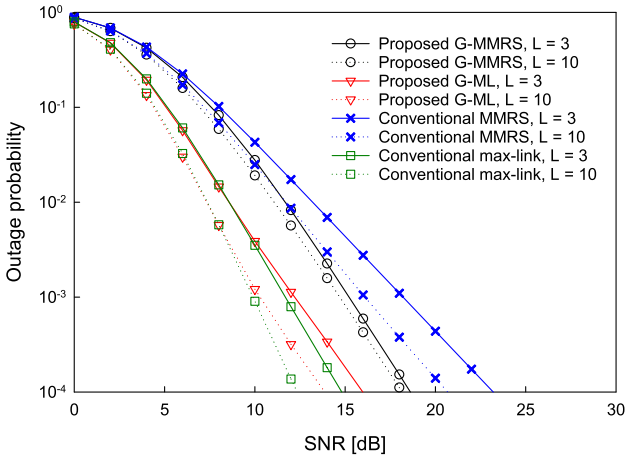

FIGURE 5. Outage probabilities of the proposed G-MMRS, the proposed G-ML, the conventional MMRS, and the conventional max–link schemes, having $K = 3$ relay nodes, where the buffer size L of each relay node was set to $L = 3$ and 10.

from the source node. First, Fig. 4 shows the outage probability of the two proposed protocols and the two benchmark protocols, each considering $K = 2$ relay nodes with ($L = 2$)-sized buffers. The theoretical outage probabilities of the proposed G-MMRS and G-ML protocols, which are derived in Sections IV-A and IV-B, were plotted, while those of the conventional MMRS and max–link protocols were calculated according to [5] and [21], respectively. As shown in Fig. 4, the theoretical and simulation curves of each of the four protocols were in agreement, thereby validating the obtained simulation results. More specifically, the proposed G-MMRS protocol exhibited a higher diversity order and a better outage probability than the conventional MMRS counterpart, while the proposed G-ML protocol was slightly outperformed by the conventional max–link counterpart in the simulated scenario.

Fig. 5 shows the outage probabilities of the four schemes, having $K = 3$ relay nodes, where the buffer size L of each relay node was set to $L = 3$ and 10. Observe in Fig. 5 that the basic performance relationship between the four schemes remained the same from the scenario of $K = 2$ relay nodes, shown in Fig. 4. For each buffer-size scenario, the proposed G-MMRS scheme exhibited a better performance than the conventional MMRS scheme, owing to its higher diversity gain, whereas the conventional max-link outperformed the proposed G-ML scheme in the high SNR regime. Since the effects of buffer overflow were included in these outage-probability calculations, the multiple packet copies at the relay nodes did not reduce the outage probability performance of the proposed G-MMRS scheme. Moreover, Fig. 5 shows that, for the proposed G-MMRS scheme, the performance difference between $L = 3$ and $L = 10$ is rather small in comparison to the two benchmark schemes.

As shown in Figs. 4 and 5, the proposed G-ML and G-MMRS schemes outperformed the MMRS scheme with regard to outage probability, whereas the max-link scheme exhibited the best outage-probability performance, which was achieved at the cost of the highest end-to-end packet delay as well as the highest overhead. Moreover, in the max-link protocol the packet delay is typically higher than in the two proposed schemes, as will be shown in Section VI-C. In order to provide further insight, the results shown in Figs. 4 and 5 were calculated under the ideal assumptions of perfect acquisition of CSI and buffer states at the destination node, as well as the assumption of IID Rayleigh block fading, which is similar to conventional studies on buffer-aided cooperative protocols. However, in a fast-fading scenario, the CSI and buffer states acquired at the destination node tend to change rapidly, and a link may be mis-selected based on the wrong CSI and buffer states. Since the overhead and the related time required for the central coordinator of the max-link protocol is the highest, as shown in Section III, the max-link protocol may severely suffer from these detrimental effects. However, a detailed investigation on this matter is beyond the scope of the present paper and is left for a future study.[7]

In order to elaborate further, we evaluated the outage performance for a slow-fading scenario, where the channel coherence time τ was longer than the packet transmission interval. Note that in other simulations we assumed the fast IID block-fading environments, which corresponded to $\tau = 1$. In Fig. 6 we compared the outage performance of the four buffer-aided schemes, which was recorded for SNR of 10 dB, while the channel coherence time was varied from $\tau = 1$ to 1000. As an additional benchmark scheme, we also plotted the outage curve of the bast relay selection (BRS)

[7]The gain of buffer-aided cooperative protocols is achieved by fully exploiting time-varying channels with the aid of data buffers at relay nodes. This implies that the gain is not attained in a static fading scenario, in which the channels remain constant. In contrast, for rapidly time-varying channels, the link selection may not be carried out correctly due to the difficulty in acquiring accurate CSI at the central coordinator.

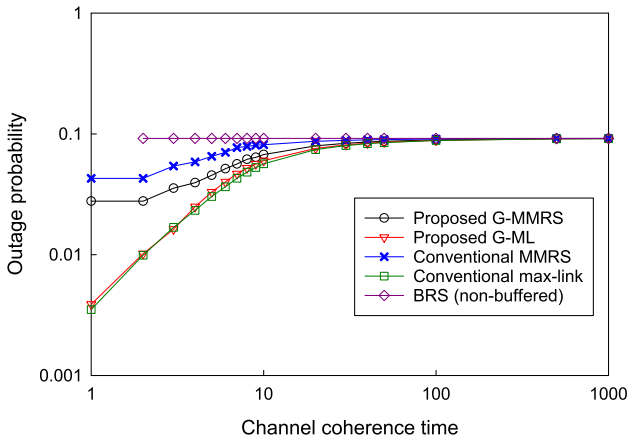

FIGURE 6. The comparisons of the outage probability for a slow-fading scenario, which was recorded for SNR of 10 dB, while the channel coherence time was varied from $\tau = 1$ to 1000.

protocol [23], which does not rely on relay node buffers. Observe in Fig. 6 that in the simulated moderate SNR scenario, the proposed G-ML scheme and the conventional max–link scheme exhibited a similar performance, which outperformed other three schemes. Furthermore, the performance advantage of the max–link protocol over the proposed and MMRS protocols became smaller, upon increasing channel coherence time. Furthermore, as predicted, the outage probabilities of all the three buffer-aided protocols converged to that of BRS protocol in the high τ limit.

B. DISTRIBUTIONS OF BUFFER STATES AT THE RELAY NODES

The distributions of the buffer states, i.e., the numbers of packets stored in the buffers of the relay nodes, are shown in Table 4, where the state transitions over 10^9 time slots were observed for SNRs of 10 dB and 20 dB. Here, the number of relay nodes is given by $K = 3$, each having an ($L = 5$)-sized buffer. The proposed G-MMRS scheme exhibited a slightly higher average buffer use than other three schemes, i.e., the proposed G-ML, the conventional MMRS, and the conventional max–link schemes, where the differences were as low as 5.3% and 13.2% for SNRs of 10 dB and 20 dB, respectively. Hence, multiple packet copies stored at the relay nodes, which is specific to the proposed scheme, does not impose a significantly high buffer usage as compared to the conventional schemes. Interestingly, the state probability corresponding to either full or empty buffers is lower in the two proposed schemes than in the two benchmark schemes. This implies that the proposed schemes have the potential of having a higher number of available links in the simulated scenario.

C. AVERAGE END-TO-END PACKET DELAY

In this section, the average end-to-end packet delays of the proposed and conventional schemes were compared by counting the number of time slots required for each source packet to arrive at the destination node. Fig. 7 shows the theoretical and numerical average end-to-end packet delays of the proposed G-ML scheme, the MMRS scheme, and the max-link scheme, where the SNR was varied from $\gamma = 0$ dB to 40 dB. The number of relay nodes was given by $K = 2$, and the buffer of each relay node was set to $L = 2$. Furthermore, infinite source-packet transmissions were considered.

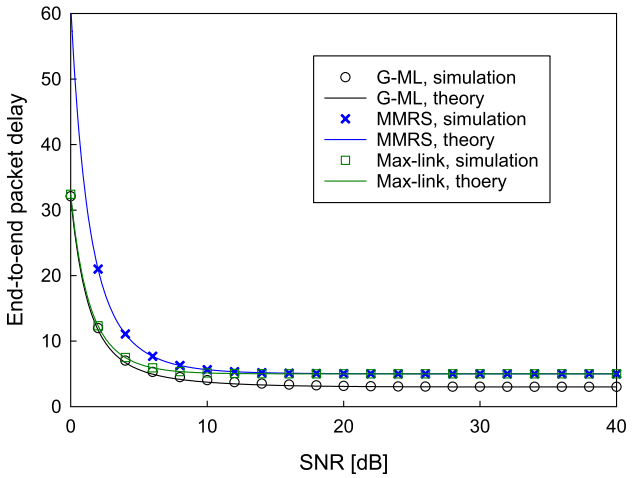

FIGURE 7. Theoretical and numerical average end-to-end packet delays of the proposed G-ML scheme, the MMRS scheme, and the max-link scheme, where the SNR was varied from $\gamma = 0$ dB to 40 dB. The number of relay nodes was given by $K = 2$, with each node having an ($L = 2$)-sized buffer. Also, the infinite source-packet transmissions were assumed.

TABLE 4. Distributions of buffer states in the simulations over 10^9 time slots for $K = 3$ relay nodes, each having an ($L = 5$)-sized buffer.

Number of stored packets	0	1	2	3	4	5	Average buffer usage
Proposed G-MMRS (SNR = 10 dB)	5.7%	16.0%	24.2%	25.5%	20.0%	8.6%	2.64
Proposed G-ML (SNR = 10 dB)	10.4%	18.6%	20.7%	20.7%	18.6%	11.0%	2.51
Conventional MMRS [4] (SNR = 10 dB)	12.6%	17.9%	19.5%	19.5%	17.9%	12.6%	2.50
Conventional max-link [5] (SNR = 10 dB)	14.5%	17.7%	17.7%	17.8%	17.8%	14.5%	2.50
Proposed GMMRS (SNR = 20 dB)	2.2%	13.4%	23.9%	25.8%	24.0%	10.7%	2.88
Proposed G-ML (SNR = 20 dB)	9.9%	19.6%	20.1%	20.3%	19.8%	10.3%	2.51
Conventional MMRS [4] (SNR = 20 dB)	11.8%	17.9%	20.3%	20.3%	17.9%	11.8%	2.50
Conventional max-link [5] (SNR = 20 dB)	14.4%	17.8%	17.8%	17.8%	17.8%	14.4%	2.50

Here, the bound of the average packet delay in the proposed G-ML protocol was calculated according to the closed-form expression of (19). Observe in Fig. 7 that the proposed G-ML protocol exhibited a lower average delay than those of the two conventional protocols. Also, the theoretical average delay curve of the G-ML protocol was a good match to its numerical counterpart.

Since the average delay profiles of infinite- and finite-source-packet transmissions typically exhibit different characteristics in the buffer-aided protocols [21], we now investigate the effects of the number of source packets $N_{\rm p}$. More specifically, in Fig. 8, the average end-to-end packet delays of the proposed G-MMRS scheme, the proposed G-ML scheme, the MMRS scheme, and the max-link scheme were recorded for an SNR of 20 dB. The number of source packets $N_{\rm p}$ per Monte Carlo simulation was varied from 10 to 10^9. The buffer size was varied from $L = 1$ to 100, and the number of relay nodes was given by $K = 3$. Note that, in order to evaluate the packet delay, the previous studies typically considered only infinite source-packet scenarios, which correspond to the packet delay of $N_{\rm p} = 10^9$ source packets, as shown in Fig. 8. Both the proposed G-MMRS and G-ML schemes exhibited an identical end-to-end packet delay in the high $N_{\rm p}$ limit of $N_{\rm p} = 10^9$, which was significantly lower than those of the two benchmark schemes. Moreover, for the scenario of $L = 50$ buffers and $N_{\rm p} = 10^5$ packets, the proposed G-MMRS scheme exhibited packet delays 9.4 and 28.8 times lower than the MMRS and max-link protocols, respectively, as expected from the information presented in Section II-E. Although the proposed G-ML scheme exhibited a higher delay profile than the proposed G-MMRS scheme, especially in the range of $N_{\rm p} = 10^3$ to 10^7, the G-ML scheme also attained a lower delay than the conventional max–link counterpart.

Next, in Fig. 9, we investigated the effects of the number of relay nodes K on the packet-delay performance, where the number of source packets ranged from $N_{\rm p} = 1$ to 100 and the SNR was maintained to be 20 dB. The buffer size was given by $L = 5$, whereas the number of relay nodes was set to $K = 3$, 4, and 5 in Figs. 9(a), 9(b), and 9(c), respectively.

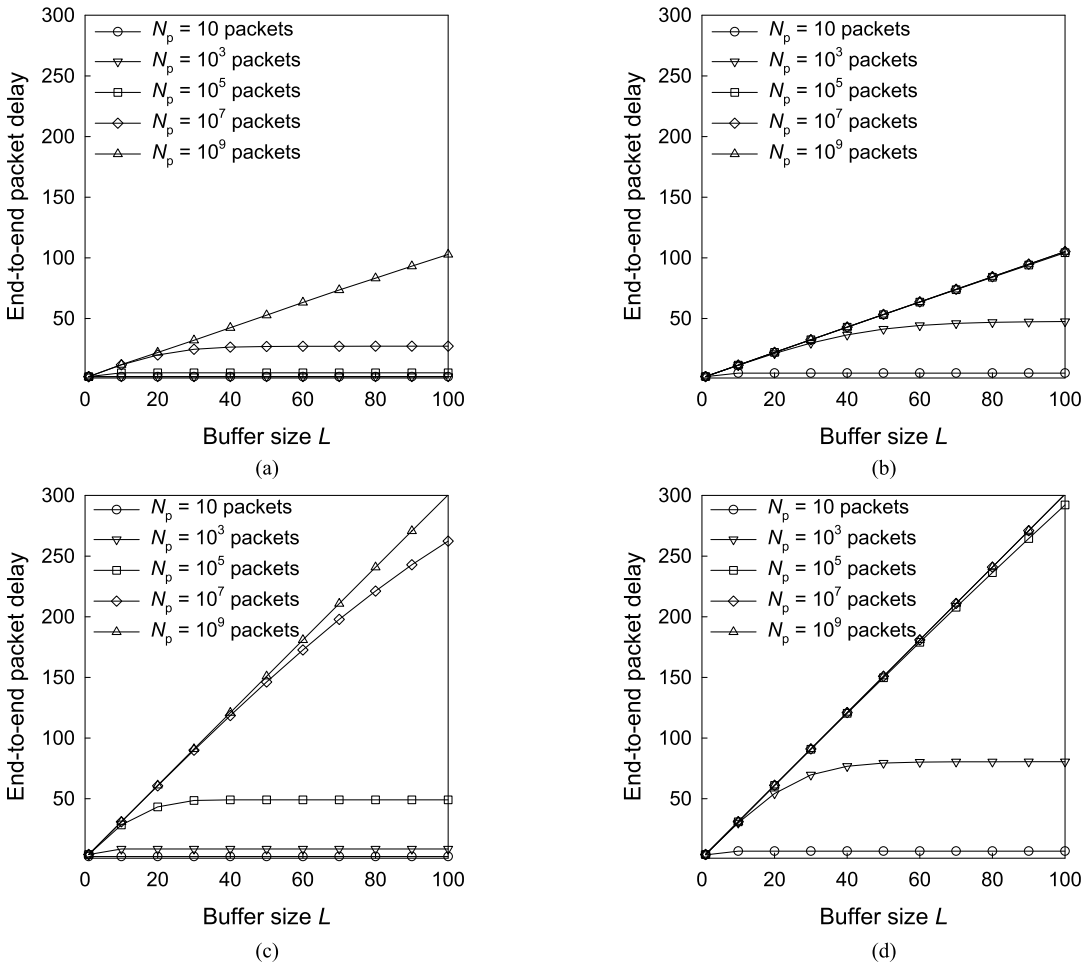

FIGURE 8. Average end-to-end packet delays of the G-MMRS, the G-ML, the MMRS, and the max–link schemes, which were recorded for an SNR of 20 dB. The number of source packets $N_{\rm p}$ was varied from 10 to 10^9. The buffer size was varied from $L = 1$ to 100, and the number of relay nodes was given by $K = 3$. (a) Proposed G-MMRS. (b) Proposed G-ML. (c) Conventional MMRS. (d) Conventional max-link.

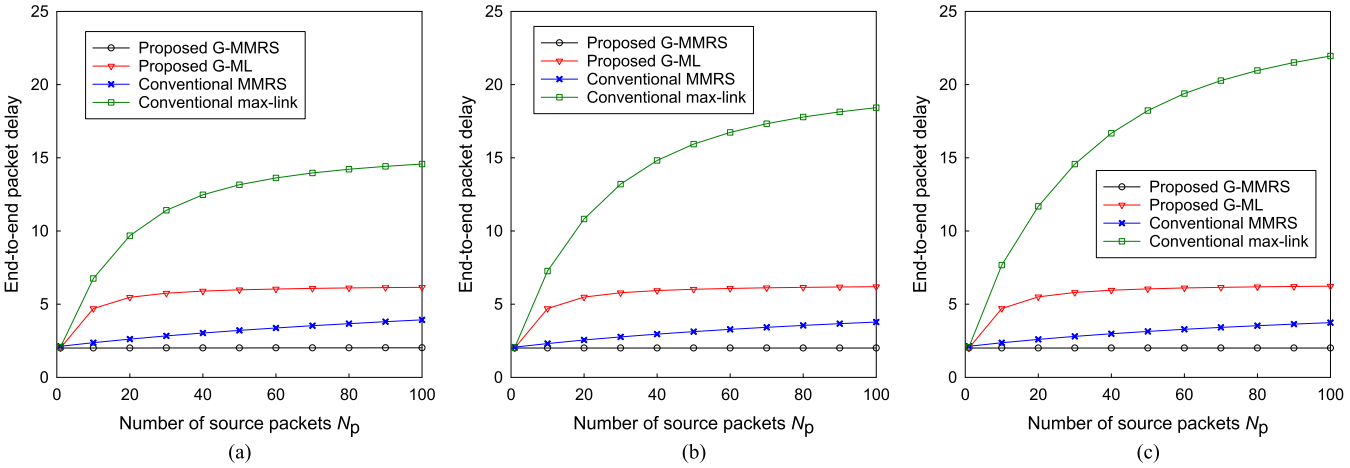

FIGURE 9. Numerical end-to-end packet delays of the four protocols considered herein, where the number of source packets ranged from $N_p = 1$ to 100 and the SNR was maintained to be 20 dB. The buffer size was given by $L = 5$, whereas the number of relay nodes was set to (a) $K = 3$, (b) $K = 4$, and (c) $K = 5$.

Regardless of the number of relay nodes K, the packet delay of the proposed G-MMRS scheme was maintained to be approximately two, which was the lowest of the four schemes. More specifically, the performance advantage of the proposed G-MMRS and G-ML schemes over the max-link protocol increased with the increase in the number of relay nodes. In order to expound a little further, while the delay profile of the two proposed protocols converged to specific values in the low number of source packets N_p, those of the two conventional protocols tended to increase upon increasing the number of packets N_p. Hence, the proposed protocols have the explicit advantage in terms of delay in the high N_p limit, as also clarified in Fig. 8.

In Fig. 10, we evaluated the effects of the average SNR on the packet delay performance of the four schemes, where the number of relay nodes was given by $K = 3$, each having an $(L = 5)$-sized buffer. The SNR was varied from $\gamma = 0$ dB to 40 dB, whereas the number of source packets N_p per Monte Carlo simulation was given by $N_p = 10$, $N_p = 50$, and $N_p = 100$ in Figs. 10(a), 10(b), and 10(c), respectively. In each N_p scenario, upon increasing the SNR, the proposed G-MMRS protocol converged to the minimum delay of two time slots, while outperforming two other benchmark schemes. More specifically, in the moderate SNR regime of $5 \leq \gamma \leq 30$ dB, the proposed G-MMRS scheme exhibited an explicit advantage over the MMRS protocol. Furthermore, the max-link protocol typically converged to a packet delay that was several times higher than that of the proposed G-MMRS and G-ML protocols. Upon increasing N_p, this performance gap increased.

Having investigated the proposed protocols' performance in symmetric channels, we now briefly investigate the effects of asymmetric channels on the performance of the proposed protocols. Fig. 11 shows the average packet delays of the

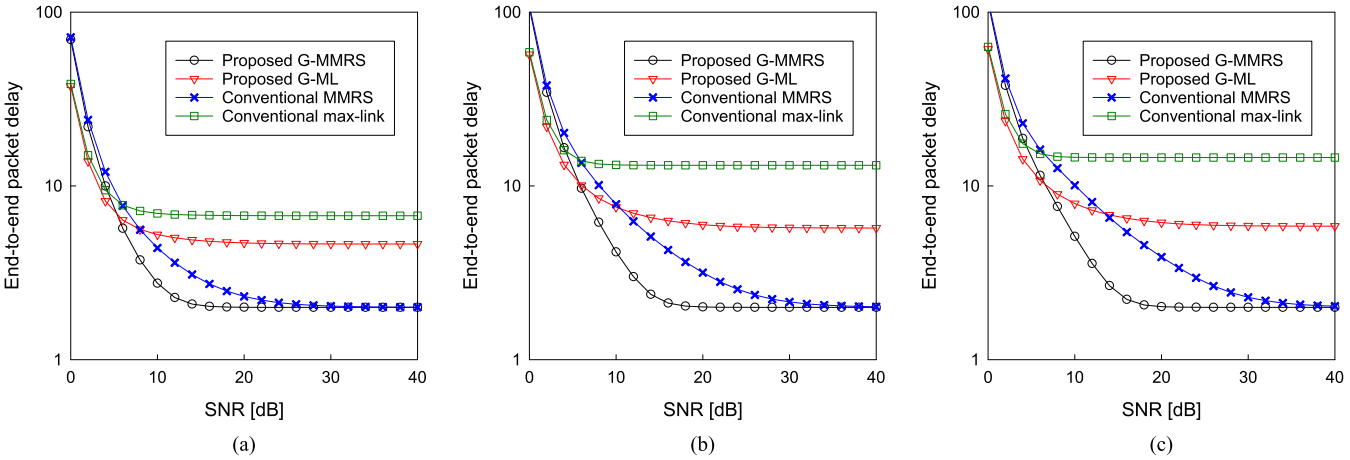

FIGURE 10. Average end-to-end packet delays of the proposed G-MMRS scheme, the proposed G-ML scheme, the MMRS scheme, and the max-link scheme, where the SNR was varied from $\gamma = 0$ dB to 40 dB. The number of relay nodes was given by $K = 3$, with each node having an $(L = 5)$-sized buffer. The number of source packets N_p per Monte Carlo simulation was given by (a) $N_p = 10$, (b) $N_p = 50$, and (c) $N_p = 100$.

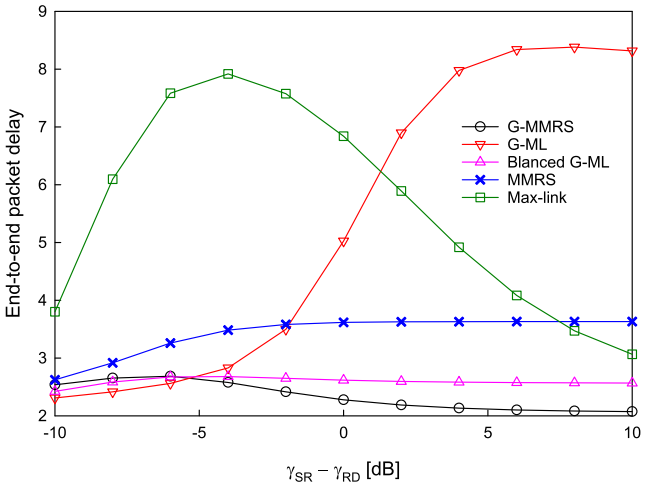

FIGURE 11. The average packet delays of the G-MMRS protocol, the G-ML protocol, the balanced G-ML protocol with the parameter of $P_C = 80\%$, the MMRS protocol, and the max-link protocol, experiencing asymmetric channels, where the SNR gap $\alpha = \gamma_{SR} - \gamma_{RD}$ was varied from -10 to 10 dB. The number of relay nodes and the buffer size were given by $K = 3$ and $L = 5$, respectively. Also, the number of source packets was given by $N_p = 10$, while the SNR of RD links was maintained to be $\gamma_{RD} = 12$ dB.

G-MMRS, the G-ML, the balanced G-ML, the max-link, and the MMRS schemes. The parameter P_C of the balanced G-ML protocol was given by $P_C = 80\%$, while the number of relay nodes was $K = 3$, each having the buffer of $L = 5$. Here, we considered the relationship between the average SNRs of SR links γ_{SR} and those of RD links γ_{RD} as follows:

$$\gamma_{SR} = \gamma_{RD} + \alpha. \tag{20}$$

The SNR gap α was varied from -10 to 10 dB, while the average SNR of the RD links was maintained to be $\gamma_{RD} = 12$ dB. Furthermore, the number of source packets was given by $N_p = 10$. As seen in Fig. 11, the G-MMRS and the balanced G-ML protocols exhibited the similar packet delays, which were lower than those of other MMRS and max-link benchmark schemes.

VII. CONCLUSIONS

In the present paper, we proposed two novel buffer-aided cooperative schemes that, in contrast to that of the conventional buffer-aided protocols relying on a single link per time slot, exploit the multiple links between a single source node and multiple relay nodes in a simultaneous manner. Thus, the proposed concept introduces an additional degree of freedom into the system design of buffer-aided protocols. As its explicit benefits, both the two proposed G-MMRS and G-ML protocols attained the significantly lower packet delay than the conventional MMRS and max–link counterparts. Furthermore, in the G-MMRS protocol the overhead required for monitoring the SR channels is eliminated, and hence the G-MMRS protocol exhibits approximately four times lower overhead than the conventional max–link protocol. The theoretical and numerical analyses of the present study demonstrated that the proposed protocols achieve both reduced overhead and packet delay, while maintaining the high diversity gain specific to the buffer-aided protocol.

REFERENCES

[1] B. Xia, Y. Fan, J. Thompson, and H. V. Poor, "Buffering in a three-node relay network," *IEEE Trans. Wireless Commun.*, vol. 7, no. 11, pp. 4492–4496, Nov. 2008.
[2] R. Wang, V. K. N. Lau, and H. Huang, "Opportunistic buffered decode-wait-and-forward (OBDWF) protocol for mobile wireless relay networks," *IEEE Trans. Wireless Commun.*, vol. 10, no. 4, pp. 1224–1231, Apr. 2011.
[3] N. B. Mehta, V. Sharma, and G. Bansal, "Performance analysis of a cooperative system with rateless codes and buffered relays," *IEEE Trans. Wireless Commun.*, vol. 10, no. 4, pp. 1069–1081, Apr. 2011.
[4] A. Ikhlef, D. S. Michalopoulos, and R. Schober, "Max-max relay selection for relays with buffers," *IEEE Trans. Wireless Commun.*, vol. 11, no. 3, pp. 1124–1135, Mar. 2012.
[5] I. Krikidis, T. Charalambous, and J. S. Thompson, "Buffer-aided relay selection for cooperative diversity systems without delay constraints," *IEEE Trans. Wireless Commun.*, vol. 11, no. 5, pp. 1957–1967, May 2012.
[6] C. Dong, L.-L. Yang, and L. Hanzo, "Performance analysis of multihop-diversity-aided multihop links," *IEEE Trans. Veh. Technol.*, vol. 61, no. 6, pp. 2504–2516, Jul. 2012.
[7] N. Zlatanov, R. Schober, and P. Popovski, "Buffer-aided relaying with adaptive link selection," *IEEE J. Sel. Areas Commun.*, vol. 31, no. 8, pp. 1530–1542, Aug. 2013.
[8] H. Liu, P. Popovski, E. de Carvalho, and Y. Zhao, "Sum-rate optimization in a two-way relay network with buffering," *IEEE Commun. Lett.*, vol. 17, no. 1, pp. 95–98, Jan. 2013.
[9] T. Islam, A. Ikhlef, R. Schober, and V. K. Bhargava, "Diversity and delay analysis of buffer-aided BICM-OFDM relaying," *IEEE Trans. Wireless Commun.*, vol. 12, no. 11, pp. 5506–5519, Nov. 2013.
[10] N. Zlatanov, A. Ikhlef, T. Islam, and R. Schober, "Buffer-aided cooperative communications: Opportunities and challenges," *IEEE Commun. Mag.*, vol. 52, no. 4, pp. 146–153, Apr. 2014.
[11] Z. Tian, G. Chen, Y. Gong, Z. Chen, and J. Chambers, "Buffer-aided max-link relay selection in amplify-and-forward cooperative networks," *IEEE Trans. Veh. Technol.*, vol. 64, no. 2, pp. 553–565, Feb. 2015.
[12] C. Dong, L.-L. Yang, and L. Hanzo, "Multi-hop diversity aided multi-hop communications: A cumulative distribution function aware approach," *IEEE Trans. Commun.*, vol. 61, no. 11, pp. 4486–4499, Nov. 2013.
[13] C. Dong, L.-L. Yang, J. Zuo, S. X. Ng, and L. Hanzo, "Energy, delay, and outage analysis of a buffer-aided three-node network relying on opportunistic routing," *IEEE Trans. Commun.*, vol. 63, no. 3, pp. 667–682, Mar. 2015.
[14] S. Huang, J. Cai, and H. Zhang, "Relay selection for average throughput maximization in buffer-aided relay networks," in *Proc. IEEE Int. Conf. Commun.*, London, U.K., Jun. 2015, pp. 3597–3601.
[15] S. Luo and K. Teh, "Buffer state based relay selection for buffer-aided cooperative relaying systems," *IEEE Trans. Wireless Commun.*, vol. 14, no. 10, pp. 5430–5439, Oct. 2015.
[16] C. Dong, L. Li, B. Zhang, L. L. Yang, and L. Hanzo, "Energy dissipation versus delay tradeoffs in a buffer-aided two-hop link," *IEEE Trans. Veh. Technol.*, to be published.
[17] J. N. Laneman and G. W. Wornell, "Distributed space-time-coded protocols for exploiting cooperative diversity in wireless networks," *IEEE Trans. Inf. Theory*, vol. 49, no. 10, pp. 2415–2425, Oct. 2003.
[18] R. U. Nabar, H. Bolcskei, and F. W. Kneubuhler, "Fading relay channels: Performance limits and space-time signal design," *IEEE J. Sel. Areas Commun.*, vol. 22, no. 6, pp. 1099–1109, Aug. 2004.
[19] S. Sugiura, S. Chen, H. Haas, P. M. Grant, and L. Hanzo, "Coherent versus non-coherent decode-and-forward relaying aided cooperative space-time shift keying," *IEEE Trans. Commun.*, vol. 59, no. 6, pp. 1707–1719, Jun. 2011.
[20] Q. Li, Q. Yan, K. C. Teh, K. H. Li, and Y. Hu, "A multi-relay-selection scheme with cyclic delay diversity," *IEEE Commun. Lett.*, vol. 17, no. 2, pp. 349–352, Feb. 2013.
[21] M. Oiwa, C. Tosa, and S. Sugiura, "Theoretical analysis of hybrid buffer–aided cooperative protocol based on max–max and max–link relay selections," *IEEE Trans. Veh. Technol.*, to be published.
[22] V. Jamali, N. Zlatanov, A. Ikhlef, and R. Schober, "Achievable rate region of the bidirectional buffer-aided relay channel with block fading," *IEEE Trans. Inf. Theory*, vol. 60, no. 11, pp. 7090–7111, Nov. 2014.

[23] A. Bletsas, A. Khisti, D. P. Reed, and A. Lippman, "A simple cooperative diversity method based on network path selection," *IEEE J. Sel. Areas Commun.*, vol. 24, no. 3, pp. 659–672, Mar. 2006.
[24] A. Ikhlef, J. Kim, and R. Schober, "Mimicking full-duplex relaying using half-duplex relays with buffers," *IEEE Trans. Veh. Technol.*, vol. 61, no. 7, pp. 3025–3037, Sep. 2012.
[25] I. Ahmed, A. Ikhlef, R. Schober, and R. K. Mallik, "Power allocation for conventional and buffer-aided link adaptive relaying systems with energy harvesting nodes," *IEEE Trans. Wireless Commun.*, vol. 13, no. 3, pp. 1182–1195, Mar. 2014.
[26] G. Chen, Z. Tian, Y. Gong, Z. Chen, and J. A. Chambers, "Max-ratio relay selection in secure buffer-aided cooperative wireless networks," *IEEE Trans. Inf. Forensics Security*, vol. 9, no. 4, pp. 719–729, Apr. 2014.
[27] V. Jamali, N. Zlatanov, and R. Schober, "Bidirectional buffer-aided relay networks with fixed rate transmission–Part I: Delay-unconstrained case," *IEEE Trans. Wireless Commun.*, vol. 14, no. 3, pp. 1323–1338, Mar. 2015.
[28] V. Jamali, N. Zlatanov, and R. Schober, "Bidirectional buffer-aided relay networks with fixed rate transmission–Part II: Delay-constrained case," *IEEE Trans. Wireless Commun.*, vol. 14, no. 3, pp. 1339–1355, Mar. 2015.
[29] M. Oiwa and S. Sugiura, "On the simultaneous exploitation of multiple source-to-relay channels in buffer–aided two-hop cooperative networks," in *Proc. IEEE 83rd Veh. Technol. Conf. (VTC-Spring)*, Nanjing, China, May 2016, pp. 1–5.
[30] W. E. Ryan and S. Lin, *Channel Codes: Classical and Modern*. Cambridge, U.K.: Cambridge Univ. Press, 2009.
[31] N. Zlatanov and R. Schober, "Buffer-aided relaying with adaptive link selection—Fixed and mixed rate transmission," *IEEE Trans. Inf. Theory*, vol. 59, no. 5, pp. 2816–2840, May 2013.
[32] S. Cui, A. J. Goldsmith, and A. Bahai, "Energy-efficiency of MIMO and cooperative MIMO techniques in sensor networks," *IEEE J. Sel. Areas Commun.*, vol. 22, no. 6, pp. 1089–1098, Aug. 2004.
[33] J. D. C. Little and S. C. Graves, *Building Intuition: Insights from Basic Operations Management Models and Principles*. Boston, MA, USA: Springer, 2008, pp. 81–100.

MIHARU OIWA (S'16) was born in Tsukuba, Japan, in 1994. She received the B.E. degree in computer and information sciences from the Tokyo University of Agriculture and Technology, Koganei, Japan, in 2016. She is currently pursuing the Ph.D. degree with the Department of Computer and Information Sciences, Tokyo University of Agriculture and Technology. Her research interests are in cooperative wireless communications and networks. She received the IEEE VTS Tokyo Chapter 2016 Young Researcher's Encouragement Award.

SHINYA SUGIURA (M'06–SM'12) received the B.S. and M.S. degrees in aeronautics and astronautics from Kyoto University, Kyoto, Japan, in 2002 and 2004, respectively, and the Ph.D. degree in electronics and electrical engineering from the University of Southampton, Southampton, U.K., in 2010. From 2004 to 2012, he was a Research Scientist with Toyota Central Research and Development Laboratories, Inc., Aichi, Japan. Since 2013, he has been an Associate Professor with the Department of Computer and Information Sciences, Tokyo University of Agriculture and Technology, Tokyo, Japan, where he heads the Wireless Communications Research Group. His research has covered a range of areas in wireless communications, networking, signal processing, and antenna technology. He has authored or co-authored over 70 refereed research publications, including 44 IEEE journal and magazine papers. He was a recipient of a number of awards, including the Young Scientists' Prize by the Minister of Education, Culture, Sports, Science and Technology of Japan in 2016, the 14th Funai Information Technology Award (First Prize) from the Funai Foundation in 2015, the 28th Telecom System Technology Award from the Telecommunications Advancement Foundation in 2013, the Sixth IEEE Communications Society Asia-Pacific Outstanding Young Researcher Award in 2011, the 13th Ericsson Young Scientist Award in 2011, and the 2008 IEEE Antennas and Propagation Society Japan Chapter Young Engineer Award. He was also certified as an Exemplary Reviewer of the IEEE COMMUNICATIONS LETTERS in 2013 and 2014.